

Ocean bays surrounded by desert land could support photosynthetic life on Snowball Earth

Greta E. M. Shum¹, Marysa M. Laguë², Abigail L.S. Swann¹, Cecilia Bitz¹, Edwin D Waddington¹, and Stephen G. Warren¹

¹University of Washington

²University of Utah

March 27, 2024

Abstract

Photosynthetic eukaryotic algae survived the Neoproterozoic Snowball Earth events, indicating that liquid-water refugia existed somewhere on the surface. We examine the potential for refugia at the coldest time of a snowball event, before CO₂ had risen and with high-albedo ice on the frozen ocean, before it became darkened by dust deposition. We use the Community Earth System Model to simulate a “modern” Snowball Earth (i.e., with continents in their current configuration), in which the ocean surface has frozen to the equator as “sea glaciers”, hundreds of meters thick, flowing like ice shelves. Despite global mean surface temperatures below -60°C, some areas of the land surface reach above-freezing temperatures because they are darker than the ice-covered ocean. With low CO₂ (10 ppm) and land-surface albedo 0.4 (characteristic of bright sand-deserts), 0.1 percent of the land surface could host liquid water seasonally; this increases to 12 percent for darker land of albedo 0.2, characteristic of polar deserts. Narrow bays intruding from the ocean to these locations (such as the modern Red Sea) could provide a water source protected from sea-glacier invasion, where photosynthetic life could survive. The abundance of potential refugia increases more strongly in response to reducing the land albedo than to increasing the CO₂, for the same global radiative forcing.

1 **Ocean bays surrounded by desert land could support photosynthetic life on**
2 **Snowball Earth**

3
4 Greta E.M. Shum^{1,2,*}, Marysa M. Laguë³, Abigail L.S. Swann^{1,4}, Cecilia M. Bitz^{1,2},
5 Edwin D. Waddington⁵, and Stephen G. Warren^{1,2,5}

6
7 ¹Department of Atmospheric Sciences, University of Washington, Seattle, WA 98195, USA.

8 ²Astrobiology Program, University of Washington Seattle, WA 98195, USA.

9 ³Department of Atmospheric Sciences, University of Utah, Salt Lake City, UT 84112, USA.

10 ⁴Department of Biology, University of Washington, Seattle, WA 98195, USA.

11 ⁵Department of Earth and Space Sciences, University of Washington, Seattle, WA 98195, USA.

12
13 For submission to *AGU Advances*

14 21 March 2024

15
16 *Corresponding author. Email: gshum@uw.edu
17

18 **Key points:**

- 19 • Snow-free desert land (with albedo lower than the frozen ocean) can warm the local climate.
20 • Lowering land-surface albedo expands the area of net-sublimating, snow-free land.
21 • Numerous narrow-bay refugia for photosynthetic life (places with surface temperatures above
22 freezing) can exist on Snowball Earth.

23
24 **Keywords:** Snowball Earth, sea ice, albedo, sea glacier, radiative forcing, refugia

25 **Abstract**

26 Photosynthetic eukaryotic algae survived the Neoproterozoic Snowball Earth events, indicating
27 that liquid-water refugia existed somewhere on the surface. We examine the potential for refugia
28 at the coldest time of a snowball event, before CO₂ had risen and with high-albedo ice on the
29 frozen ocean, before it became darkened by dust deposition. We use the Community Earth
30 System Model to simulate a “modern” Snowball Earth (i.e., with continents in their current
31 configuration), in which the ocean surface has frozen to the equator as “sea glaciers”, hundreds
32 of meters thick, flowing like ice shelves. Despite global mean surface temperatures below -60°C,
33 some areas of the land surface reach above-freezing temperatures because they are darker than
34 the ice-covered ocean. With low CO₂ (10 ppm) and land-surface albedo 0.4 (characteristic of
35 bright sand-deserts), 0.1 percent of the land surface could host liquid water seasonally; this
36 increases to 12 percent for darker land of albedo 0.2, characteristic of polar deserts. Narrow bays
37 intruding from the ocean to these locations (such as the modern Red Sea) could provide a water
38 source protected from sea-glacier invasion, where photosynthetic life could survive. The
39 abundance of potential refugia increases more strongly in response to reducing the land albedo
40 than to increasing the CO₂, for the same global radiative forcing.

41 **Plain language summary**

42 Two “Snowball Earth” events occurred approximately 600 million years ago, when the shape
43 and location of continents were different from today. During these events, the ocean was
44 apparently covered with “sea glaciers”, hundreds of meters thick, which flowed like ice shelves.
45 Yet photosynthetic algae survived these events, indicating that small regions of liquid water
46 (“refugia”) existed somewhere on the surface. An Earth System Model shows that, even with
47 global average surface temperature below -60°C , some areas of the land surface reach above-
48 freezing temperatures because they are darker than the ice-covered ocean. Narrow bays intruding
49 from the ocean to these locations (such as the modern Red Sea) could provide a water source
50 protected from sea-glacier invasion, where photosynthetic life could survive.

51 **1. Introduction**

52 On Earth and Earth-like worlds, a large negative radiative forcing can initiate a positive ice-
53 albedo feedback and ultimately lead to global glaciation (Budyko, 1969; Sellers, 1969). Geologic
54 evidence indicates that the Earth has experienced several such events since the emergence of life
55 (Harland, 1964; Kirschvink, 1992; Hoffman et al., 2017; Evans, 2000). These events were likely
56 caused by a reduction of the atmospheric greenhouse effect, resulting from disturbance of the
57 global carbon cycle (Hoffman et al., 2017). During the Neoproterozoic era (600-800 Ma), two
58 “Snowball Earth” events occurred: the Sturtian, with a duration of 58 million years, and the
59 Marinoan, with a duration of ~10 million years (Macdonald et al., 2010). The oceans would
60 likely have been covered by ice hundreds of meters thick, but photosynthetic eukaryotic algae
61 were able to survive (Porter, 2004; Knoll, 2011, 2014), indicating that some liquid water was
62 maintained at or near the surface where light was available for photosynthesis.

63 In this paper, we focus on the “hard” Snowball Earth, in which the equatorial ocean would be
64 covered by thick ice. That ice differed in several ways from sea ice on the polar oceans of
65 modern Earth. Modern sea-ice thickness is limited to a few meters by summertime melting and
66 by a heat flux F_0 of several watts per square meter from the ocean water below, which originally
67 gained its heat by absorption of solar energy at lower latitudes. But at the onset of a snowball
68 event, when sea ice reached the equator it would shut off solar heating of the ocean water below.
69 After a few thousand years, the ocean would have lost its reservoir of heat, leaving only
70 geothermal heat, $F_0 \approx 0.08 \text{ W m}^{-2}$ (about one-hundredth that of the modern oceanic flux F_0 to the
71 ice bottom), increasing the equilibrium ice thickness from a few meters to a few hundred meters
72 (Warren et al., 2002).

73 The geothermal flux is essentially independent of latitude, but the ice surface on the snowball
74 ocean would be colder at high latitude than at low latitude, resulting in thicker ice at higher

75 latitude. The latitudinal thickness gradient would cause the ice to flow (Goodman and
76 Pierrehumbert, 2003). In this state, the thick ice on the frozen ocean would be growing from
77 above by snowfall (the original sea ice having melted off the bottom), and therefore can be
78 classified as glacier ice rather than sea ice. This ice, flowing like the modern Antarctic ice
79 shelves but not dependent on continental glaciation, is called a *sea glacier* (Warren et al., 2002).
80 Sea glaciers are computed to flow as much as 7-50 meters per year even when they cover the
81 entire ocean (Goodman, 2006; Li & Pierrehumbert, 2011). If a small area of the ocean were to
82 open up, it would be quickly filled by inflow of the sea glacier. How, then, could liquid water be
83 maintained at the surface? Several hypotheses for refugia have been proposed, which we now
84 list.

85

86 ***1.1. Types of proposed refugia***

87 Five ideas have been proposed for liquid-water refugia at the ocean surface.

88 (a) ***Hotspots***. Hoffman and Schrag (2000, 2002) noted that geological hotspots at the ocean
89 floor under shallow water, as occur near the coasts of Hawaii and Iceland, would melt inflowing
90 ice fast enough to maintain pools of liquid seawater. These pools would be small in area, and
91 would not be stable for millions of years, so any life would have to survive many long and deep
92 migrations.

93 (b) ***Thin ice***. McKay (2000), using a broadband model for solar radiation, proposed that
94 absorption of sunlight within the ice might be able to limit the tropical ice thickness to ~10 m.
95 Warren et al. (2002) pointed out that the visible and ultraviolet wavelengths, which penetrate
96 deeply, are not absorbed but eventually are scattered back out to space, whereas the near-infrared
97 wavelengths, which are indeed absorbed, are absorbed in the top few millimeters, so their heat is
98 easily conducted up to the atmosphere. By modifying McKay's model to compute the radiation

99 spectrally, Warren et al. found that the equilibrium ice thickness in a typical example grew from
100 1 m to 800 m. McKay joined as a coauthor on that paper, agreeing that the thin-ice solution was
101 not viable. Pollard and Kasting (2005) tried to find a thin-ice solution that would even hold off
102 sea glaciers, and succeeded only when three parameters were pushed beyond their acceptable
103 limits (Warren and Brandt, 2006). An improved model (Pollard et al., 2017) convincingly
104 rejected the thin-ice solution.

105 **(c) Waterbelt.** Some models of snowball initiation have found that sea ice could reach the
106 outer tropics but still leave a wide belt of open water centered on the equator, spanning tens of
107 degrees of latitude and circling the globe, if the sea-ice (or sea-glacier) albedo is low enough.
108 Abbot, Voigt, and Koll (2011) found that this “waterbelt” state could exist with sea-glacier
109 albedo of 0.45 but is inaccessible for sea-glacier albedo >0.55 . Dacic et al.’s (2013)
110 measurements of modern surrogates for sea-glacier surfaces found albedos 0.57-0.80 under clear
111 sky, and even higher under cloudy sky, arguing against the waterbelt idea. A follow-on
112 investigation by Voigt’s group (Braun et al., 2022) found the waterbelt to be unviable, even with
113 sea-glacier albedo as low as 0.45. Most recently, Hörner and Voigt (2023) showed that the
114 waterbelt in earlier models resulted from inadequate vertical resolution in the sea ice.

115 **(d) Ice surface.** Vincent and Howard-Williams (2000), and Vincent et al. (2000), suggested
116 that microbial life could survive on the ice surface of Snowball Earth, pointing to the widespread
117 microbial communities that thrive both in surface meltwater pools and in brine pockets, on
118 modern Arctic and Antarctic sea ice and ice shelves. These communities can persist even if only
119 a few days per year have temperatures above freezing. Such communities could indeed have
120 been active during the rapid advance of sea ice at the onset of Snowball Earth. But after the ice
121 reaches the equator, the strong positive albedo-temperature feedback causes dramatic cooling.
122 An early general circulation model (GCM) of the hard snowball by Pollard and Kasting (2004)

123 obtained a global average surface temperature of -49°C . The warmest temperature on the ocean
124 surface was found on a summer afternoon in the subtropics, $\sim -30^{\circ}\text{C}$, which seemed to rule out
125 any surface life. However, we will see below that Vincent's proposal can be resurrected if it is
126 considered in combination with the next proposed refugium (*e*).

127 (*e*) **Narrow bay.** One place where ocean water could be safe from sea-glacier inflow is at
128 the innermost end of a narrow bay resulting from continental rifting, like the modern Red Sea.
129 When flowing into a narrow bay, nearly enclosed by dry land, ice flow can be slowed by
130 resistive shear stresses from the side-walls, and by obstacles such as islands, shoals, or narrows
131 in the bay. If the bay is long enough and the sublimation rate is high enough, the ice thickness
132 can taper down to zero before the end of the bay is reached (Campbell et al., 2011, 2014). To
133 illuminate these concepts, in the Appendix we derive a characteristic penetration distance based
134 on a simplified sea glacier in a simplified bay, in the absence of geometric complexities. If
135 ocean-sourced water flowing under the ice can find its way to the end of the narrow bay, it could
136 provide a refugium safe from sea glaciers. If the surrounding land is net-evaporative (i.e.,
137 potential sublimation outpaces precipitation, as in deserts), this place would be safe from land
138 glaciers as well.

139 Refugia in narrow bays would be larger than the isolated geothermal hotspots around
140 volcanic islands, and would have long lifetimes, similar to timescales of continental drift. But
141 even if the end of the bay is safe from sea-glacier inflow, there is the risk that the climate might
142 still be so cold that thick sea ice would grow locally. Such a refugium would be feasible only if
143 local temperatures reach above freezing, which could occur because the albedo of nearby bare
144 land surfaces would be lower than that of the ice-covered ocean. Land surfaces during the
145 Snowball Earth events were not vegetated: possible snow-free surfaces would be bare rock, bare
146 soil, and sand. Most of them are brighter than vegetated land, but with albedos 0.1-0.4 they are

147 much darker than ice or snow. To evaluate the feasibility of this refugium, climate modeling is
148 needed, and that is the subject of this paper.

149

150 **2. Investigation of the ocean-bay refugium**

151 Given the high uncertainty of Neoproterozoic paleocontinental reconstructions, for this
152 investigation we apply an earth-system model to the *modern* continental configuration. This
153 approach has been used in prior investigations, called “modern Snowball Earth” (Voigt and
154 Marotzke, 2010; Liu et al., 2018). It has the advantage of familiar geography, allowing
155 comparisons of atmospheric circulation and climate with the familiar regional climates of the
156 present. We take the modern continental configuration as a representative arrangement of
157 continents of various size and shape, scattered across a range of latitudes.

158 As potential refugia, in addition to nearly-enclosed seas such as the Red Sea and
159 Mediterranean, we also seek locations on land where the local temperature exceeds the freezing
160 point of seawater at least once during the year; i.e. $T_{max} > -2^{\circ}\text{C}$. With the right coastline geometry
161 in a paleocontinental configuration (to allow for ocean-water access), these locations would be
162 potential oases for photosynthetic eukaryotes.

163 Continental positioning itself is uncertain, and coastline geometry of the Neoproterozoic is
164 even more uncertain. The period was tectonically active, and thus we make an explicit
165 assumption that narrow bays are likely to have occurred and therefore seasonally above-freezing
166 temperatures on land in our “modern Snowball Earth” allow for potential refugia even if these
167 areas are not currently near a modern narrow bay. Additionally, many narrow bays would be
168 smaller than the resolution of a typical global Earth System Model; thus, we focus on land
169 surface temperatures as an indicator of possible refugia. To investigate whether life could survive
170 the harshest conditions of the Snowball climate, in this paper we test the hypothesis that above-

171 freezing land temperatures can exist in an Earth System Model in the “hard” Snowball Earth
172 limit, in which even the tropical oceans are covered by ice hundreds of meters thick (no
173 waterbelt).

174 The name “snowball” is somewhat misleading, in that the ocean was not entirely snow-
175 covered. On the modern Earth, evaporation (E) exceeds precipitation (P) over nearly half the
176 ocean, mostly in the subtropics. A large region of negative $P-E$ would also have existed on the
177 Snowball Earth, according to general circulation models, although the hydrological cycle was
178 probably weakened by a factor of ~ 30 (Pollard and Kasting, 2004). At high and middle latitudes
179 the sea glaciers would have been covered by thick snow. But as sea glaciers flowed equatorward
180 into the tropical region of net sublimation, their surface snow (albedo ~ 0.8) would sublimate
181 away, exposing old snow (“firn”, albedo ~ 0.7). Then the firn would likewise sublimate away,
182 exposing bare glacier ice (albedo ~ 0.6) to the atmosphere and to solar radiation. These albedos
183 were measured on modern surrogates in the Allan Hills of East Antarctica: firn and glacier ice
184 exposed by sublimation, which have never experienced melting (Figure 1 and Table 1) (Dadic et
185 al., 2013).

186 In our modeling we do not attempt to simulate the regional evolution of ocean surfaces from
187 snow, through firn, to glacier ice, as the sea glaciers flow equatorward. Instead, everywhere that
188 the ocean is not snow-covered, we assign its albedo to that of firn, thus biasing the global climate
189 to a cold extreme and exaggerating the difficulty of maintaining refugia. We then investigate
190 how the albedo of bare *land* surfaces, and the atmospheric CO_2 level, influence the potential
191 habitability of a snowball climate. We test a range of CO_2 levels from 10 to 200 ppm and a range
192 of uniform surface albedos for bare land from 0.2 to 0.4, using a climate model with the modern
193 continental configuration.

194 During a snowball event, volcanic CO₂ accumulates in the atmosphere because its removal
195 mechanisms (dissolving in rainwater and reacting with surface rocks) are suppressed. As the
196 climate warmed with rising atmospheric CO₂ during the progression of a snowball event, refugia
197 would have become more widespread. In addition, wind-erosion of bare land would have lifted
198 dust that could accumulate on the ice, lowering its albedo, leading to additional potential
199 mechanisms for refugia. Here we instead focus on the most extreme bottleneck of the cold early
200 phase of a snowball event, the most critical time for survival of surface life.

202 **3. Methods**

203 *3.1. Experimental Design*

204 We use a modified version of the Community Earth System Model, version 2.1.0
205 (Danabasoglu et al., 2020), with the Simple Land Interface Model (SLIM) (Laguë et al., 2019)
206 coupled to the Community Atmosphere Model, version 4 (CAM4) (Neale et al., 2010), the Los
207 Alamos sea ice model CICE5 (Hunke et al., 2015) in its thermodynamic-only mode (Bitz and
208 Lipscomb, 1999), and a slab ocean model (SOM) (Bitz et al., 2012). Ocean heat flux
209 convergence is set to zero everywhere, and sea surface temperatures are allowed to evolve.
210 Simulations are run at a nominal 2° resolution.

211 SLIM is an idealized land model, designed for assessing the interactive roles of discrete land
212 properties (e.g. bare-ground albedo, evaporative resistance, heat capacity of the soil, etc.); using
213 it allows us to directly assess the climate response of specified land-surface albedos. Heat
214 diffusion in the model is represented on a vertical soil grid that is separate from the water budget.
215 Hydrology is represented using a simple bucket model that combines a user-specified “lid”
216 resistance with a resistance related to the fill level of the water bucket. Snow can accumulate on
217 the surface, and can be removed by sublimation to the atmosphere or melting into the land. The

218 model solves a linearized surface energy budget to calculate surface temperature, surface fluxes
219 of radiation, turbulent heat fluxes, and ground heat storage.

220 When snow falls on the surface of land or sea ice, it masks the albedo of the underlying
221 surface. On land, snow masks the albedo of bare ground when it exceeds a mass of 10 kg/m^2
222 liquid-equivalent (about 3 to 10 cm of snow, for typical snow densities $0.1\text{-}0.3 \text{ g cm}^{-3}$). Land-
223 surface models for the modern Earth normally use a larger snow-masking depth because of the
224 presence of grass, bushes, and trees, but these plants did not appear until long after the
225 Neoproterozoic snowball events.

226 In the midlatitudes and polar regions of a snowball climate, kilometer-thick ice sheets
227 covering the oceans would accumulate, thicken, and flow like modern ice shelves towards
228 thinner regions of net-sublimation as “sea glaciers” (Goodman and Pierrehumbert, 2003). It
229 would therefore be glacier ice, not sea ice, that would cover the ocean surface in a snowball
230 climate after the initial global freezing had taken place, and would have albedos ranging from
231 that of snow in areas of snow accumulation to exposed firn and finally bare glacier ice in regions
232 of net sublimation (Figure 1 and Table 1). Rather than predicting the detailed state of ice surface
233 conditions, which is typical in CICE5, for simplicity we revert back to the CCSM3 shortwave
234 radiative transfer formulation. This option allows us to prescribe “sea-ice” surface albedos. For
235 bare (snow-free) ice we set visible and near-infrared band albedos to values appropriate for firn,
236 so as to bias the global climate to its cold extreme. As snow accumulates, snow masks the bare
237 ice, and the band albedos transition to values appropriate for snow (Table 1).

238 In all simulations, sea ice is initialized with 100% concentration and 20 m thick in all ocean
239 gridcells. Sea ice rapidly grows thicker, but would take thousands of years to reach an
240 equilibrium. We do not expect sea ice ever to reach an equilibrium thickness in our simulations
241 even if we extended them, since geothermal heating is not represented; that heat source would be

242 necessary to limit the freezing of seawater to the base of thick ice (McKay, 2000; Warren et al.,
243 2002; Goodman and Pierrehumbert, 2003). Our surface temperatures could be seen as too warm.
244 For example, if the model ice thickness is only 50 m but in equilibrium would be >500 m, there
245 is an excessive conductive heat flux of 1.4 Wm^{-2} upward through the ice, causing the surface
246 temperature to be too high by $\sim 0.5 \text{ K}$.

247 Over Earth's history, the Sun has brightened by about 1% every 100 million years, so at 600
248 Ma the solar constant was $\sim 94\%$ of its present value (Crowley and Baum, 1993). That value,
249 94%, has been used to initiate the snowball state in models with Neoproterozoic continents
250 clustered at low latitude. The low-latitude land facilitates snowball initiation in those models,
251 because the albedo of bare land (0.2-0.4) exceeds that of open ocean (0.07). For a “modern”
252 Snowball Earth, with most of the continental area at middle or high latitude, a lower solar
253 constant, about 91%, is needed to initiate the snowball (Voigt and Marotzke, 2010), and that is
254 the value we use for this work.

255 In models, the critical CO_2 level required for snowball onset depends on several modeling
256 choices: sea-ice dynamics (Lewis et al, 2006; Voigt and Abbot, 2012), land topography (Liu et
257 al., 2018), continental configuration (Liu et al., 2013), mountains (Walsh et al., 2019),
258 atmospheric dust (Liu et al, 2020; Liu et al., 2021), and cloud radiative forcing (Voigt and
259 Marotzke, 2010). In prior work, modeled snowball climates have been initiated at CO_2 mixing
260 ratios as low as 2 ppm (Voigt and Abbot, 2012) and as high as 600 ppm (Liu et al., 2017) but
261 generally fall between 50 and 300 ppm, with exact values dependent on the ice coverage on sea
262 and land, the solar constant, and the land area (Schrag et al., 2002; Yang et al., 2012). For the
263 coldest early stage of a snowball event, we therefore specify a variety of CO_2 levels, along with
264 several choices for the albedo of snow-free land, and examine the resulting climatic patterns.

265 For initiation of the snowball state, we set the CO₂ mixing ratio to 100 ppm, and the albedo
266 of snow-free land to a broadband value of 0.4. The albedo of bare land (rocks or soil) increases
267 with wavelength across the solar spectrum from the ultraviolet (UV) to the infrared (IR)
268 (Figure 1). We specify the albedo in two bands: 0.3 in the UV and visible (wavelengths 0.3-0.7
269 μm), and 0.5 in the near-IR (wavelengths 0.7-5.0 μm). Under these conditions, our initial
270 simulation establishes the conditions necessary to maintain a frozen ocean in approximately 20
271 years. We run the initiation simulation for a total of 100 years to ensure that the frozen-ocean
272 state is not transient, and that the atmosphere is in steady state. Based on these conditions
273 sufficient to generate a snowball climate, further runs are initialized with a fully ice-covered
274 ocean to test the sensitivity of surface temperatures to variations in bare-land surface albedo and
275 atmospheric CO₂ concentration (details below).

276 We run the model at the global scale and thus do not resolve the fine-scale dynamics of a sea
277 glacier invading a bay. As described above, we assume that if a land gridcell experiences a
278 monthly average surface temperature that exceeds the melting point, that gridcell could
279 potentially support liquid water if a narrow arm of the sea were to reach it in a paleocontinental
280 configuration, thus rendering it a potential refugium for photosynthetic life.

281

282 ***3.2. Sampling across a range of atmospheric CO₂ concentrations and land albedos***

283 In the absence of land plants, which break up stones into sand or silt with higher albedo, the
284 Neoproterozoic land surface was probably darker than modern deserts (the fossil record suggests
285 that land plants did not evolve until 461–472 Ma (Kenrick et al., 2012; Morris et al., 2018)). The
286 highest broadband albedo for modern deserts is 0.40 for the fine sand of the Arabian Empty
287 Quarter (Smith, 1986); the lowest albedo is 0.10-0.15 for the stony desert of the western Gobi
288 (Abell et al., 2020a; Figure S1 of Abell et al. 2020b). Within this range, we test five different sets

289 of snow-free land albedo values, listed here from brightest to darkest as [UV-visible albedo/near-
290 IR albedo]: 0.3/0.5, 0.25/0.45, 0.2/0.4, 0.15/0.35, and 0.1/0.3. Approximately half the solar
291 energy is in the near-IR, so the total solar (broadband) albedo for each case is the average of the
292 two values given; i.e., 0.40, 0.35, 0.30, 0.25, 0.20. As a shorthand to identify the cases, we
293 simply give the broadband values.

294 We sample CO₂ levels of 10, 25, 50, 100, and 200 ppm. We do not test every combination of
295 albedo and CO₂ values, but we do test the edge cases, as well as the full range of albedos for a 50
296 ppm CO₂ atmosphere, and the full range of CO₂ values for land albedo 0.3 (Table 2).

297 We use the Parallel Offline Radiation Tool (PORT) (Conley et al., 2013) to calculate total
298 global radiative forcing associated with each experiment relative to a base case in the middle
299 range at CO₂ = 50 ppm and bare (snow-free) land albedo 0.3. [In Table 2 the radiative forcings
300 are shown instead relative to the coldest case (CO₂ = 10 ppm, albedo = 0.4) for ease of
301 comparison.] Table 2 shows that dropping the albedo of bare land from the brightest case (0.4) to
302 the darkest case (0.2) at 50 ppm causes a radiative forcing (RF) of 4.06 W/m², resulting in a
303 5.2 K increase in global mean surface temperature, implying a climate sensitivity of 1.28
304 K/(Wm⁻²). Increasing CO₂ from 10 ppm to 200 ppm (with land albedo 0.3) causes RF = 5.16
305 Wm⁻², and results in a temperature increase of 2.8 K, implying a lower climate sensitivity of 0.54
306 K/(Wm⁻²). These climate sensitivities may be compared to a median of 0.5 K/(Wm⁻²) in 19
307 GCMs for the modern Earth (Cess et al., 1990).

308 These climate sensitivities indicate that albedo-driven forcing kicks off stronger feedbacks
309 than CO₂-driven forcing. The snowball climate has been shown to be relatively insensitive to
310 CO₂-driven forcing; at such low temperatures, the positive feedback from the water-vapor
311 greenhouse effect is weak (Pierrehumbert 2005). Outside of the tropics, the wintertime
312 greenhouse effect is negative, resembling the modern Antarctic plateau (Sejas et al., 2018). The

313 greenhouse effect can be calculated as $G = \sigma T_S^4 - OLR$, where σ is the Stefan-Boltzmann
314 constant, and OLR is outgoing longwave radiation. Surface temperature change due greenhouse
315 warming is $\Delta T_g = T_S - [OLR/\sigma]^{1/4}$. At 50 ppm, G ranges from 0.7 W m⁻² to 2.6 W m⁻², and
316 ΔT_g , is between 0.9 and 2.3 K (higher warming at lower bare-land albedo). At 200 ppm and 0.2
317 albedo, G is 4.4 W m⁻², and ΔT_g reaches 3.5 K. Pierrehumbert (2005) obtained a similarly small
318 value for the global average on a hard snowball; their Figure 4 shows a clear-sky greenhouse
319 effect of ~8 W m⁻². These snowball values are much smaller than those for the modern Earth,
320 where $G \approx 150$ W m⁻² and $\Delta T_g = 33$ K.

321 **4. Results**

322

323 ***4.1. Some of the land surface has above-freezing mean-annual temperatures, and much more*** 324 ***has above-freezing temperatures seasonally.***

325 In our runs with lower bare-land albedo, we find small areas of land that are above-freezing
326 on annual average. These areas allow for the potential of “open water” refugia. But refugia do
327 not require open water. If the end of an oceanic bay is below freezing on annual average, but the
328 warmest month is above freezing, sea ice would form in the bay, and it would partially melt in
329 summer. Neoproterozoic algae could have survived in the temporary meltwater pools on the ice,
330 as has been observed by mat-forming eukaryotic algae on the McMurdo Ice Shelf and on the
331 Ward Hunt Ice Shelf in the Canadian Arctic (Vincent, et al., 2000; Vincent and Howard-
332 Williams, 2000). In these modern analogs, organisms can survive perennially in ice that is deeply
333 frozen for all but a few weeks or days per year. This would be the “ice surface” refugium
334 described above in Section 1.1(d).

335 We find that in our coldest case (10 ppm CO₂, bare-land albedo 0.4), 0.1% of the land
336 surface area reaches temperatures above the freezing temperature of seawater (-2°C) in at least

337 one month of the year, despite a global mean surface temperature of -69°C (Figure 2a). In our
338 warmest case (200 ppm CO_2 , bare-land albedo 0.2) in which global mean surface temperature is
339 -61°C , 17% of land surface area reaches temperatures warm enough to host liquid water in the
340 warmest month. (Our specification of the freezing temperature as -2°C is a conservative choice.
341 With perhaps 20% of the ocean water converted to land glaciers and sea glaciers, the salinity of
342 the remaining seawater would increase, lowering its freezing temperature closer to -3°C .)

343 To investigate how refugia might form, we calculate the potential evaporation (PE, mm/day),
344 a measure of the rate at which the atmosphere could evaporate or sublimate water from the
345 surface, if that surface had unlimited water availability. Over land, we calculate PE using a
346 modified version of the Penman-Monteith equation (Penman, 1948; Monteith, 1981; Scheff and
347 Frierson, 2014). Over the ocean, it is equal to the latent heat flux from the ocean to the
348 atmosphere converted to units of water flux (mm/day). The dry snowball atmosphere over land
349 creates demand for water resulting in large areas of the land surface that are snow-free for part of
350 the year (Figure 2d-f). Above-freezing land surfaces are concentrated in places where PE
351 outpaces precipitation – in particular, parts of the Arabian Peninsula, the modern Sahara Desert
352 and eastern Asia (compare Figures 2a-c and 2g-i). Without snow cover, low-albedo land absorbs
353 more solar radiation, allowing for above-freezing local land temperatures and the potential for
354 unfrozen water and refugia if an ocean bay were to intrude to those locations.

355 A net-evaporative location experiencing mean-annual temperatures above freezing may thus
356 serve as a refugium if it is connected via a narrow bay to the ocean, allowing seawater from
357 below the sublimating sea glacier to flow into the bay and replace the water lost by evaporation.

358 Our model does not represent the growth of ice sheets on land. However, we can infer that
359 snow-covered regions in Figure 2d-f are where ice sheets would grow; where they would flow
360 would depend on the land's topography. Ice sheets have been directly simulated on

361 Neoproterozoic continents (Donnadieu et al., 2003; Benn et al., 2015); they cover only parts of
362 the continents, allowing large regions to be ice-free land.

363

364 ***4.2. Land surface albedo exerts control on the habitability of nearly-enclosed bays.***

365 Land surface temperatures increase more strongly in response to decreases in bare-land
366 surface albedo than to increases in CO₂, for the same magnitude of global radiative forcing. This
367 response occurs across all latitudes and is stronger in regions with more total land area
368 (Figure 3a). Starting from a baseline of albedo 0.4 and 10 ppm CO₂, increasing CO₂ from 10 to
369 200 ppm constitutes a global radiative forcing of 5.16 Wm⁻², while decreasing snow-free land
370 albedo from 0.4 to 0.2 constitutes a smaller forcing of 4.06 Wm⁻² yet causes a greater increase of
371 warm land area. The change of land area per unit of radiative forcing is shown in Figure 3b, for
372 four cases of similar RF, two caused by increasing CO₂ and the others by decreasing albedo.
373 Despite smaller globally mean radiative forcing from albedo changes, land surface temperatures
374 are more responsive to albedo since the radiative forcing is concentrated over snow-free land.

375 Decreasing bare-land albedo facilitates potential refugia in two ways: (1) warming of bare
376 land and (2) exposing new bare land that then becomes warm. In our simulations, both
377 mechanisms occur to effect a change in habitability, with approximately 45% of the newly
378 exposed land above freezing (in the warmest month) having become warm enough to host
379 refugia through the first mechanism, and 55% through the second mechanism at constant CO₂.
380 (Partitioning is similar at 10, 50, and 200 ppm CO₂). We do not see above-freezing temperatures
381 in locations that have snow cover. If a warm, net-precipitating location did exist, it would
382 become a warm ice sheet, like a modern temperate glacier or the wet-snow zone of modern
383 Greenland.

384 Either decreasing bare-land albedo or raising CO₂ expands the area of potentially habitable
385 land in coastal gridcells; continental interiors already meet the criteria for potential habitability at
386 albedo 0.4. A world with low bare-land albedo would therefore be more likely to host life in
387 narrow bays that intrude into the dark land. As mentioned above, the bare land in the
388 Neoproterozoic probably resembled modern stony deserts rather than sand or soil, so its albedo
389 may have been even lower than the lowest case we modeled (broadband albedo 0.2).

390 Figure 4 and Table 2 show, for the various combinations of CO₂ and albedo, the percent of
391 land area capable of hosting refugia, were an arm of the sea to reach it, demonstrating again the
392 relative importance of global radiative forcing by land albedo and CO₂. Starting from the coldest
393 case (bare-land albedo 0.4, CO₂=10 ppm), positive radiative forcing results from either
394 increasing CO₂ or reducing land albedo. For the same radiative forcing, a change of land albedo
395 is more effective than a change of CO₂. Figure 4a shows this for the annual maximum
396 temperature (T_{max}); the area of above-freezing land ranges from 0.1% to 12%, by decreasing
397 bare-land albedo alone. [Even in the warmest case (bare-land albedo 0.2, CO₂=200 ppm), we do
398 not see places with *annual mean* temperature $\bar{T} > -2^{\circ}\text{C}$. That would allow for “open-water”
399 refugia, because during at least part of the year the bay would be ice-free.]

400 A temperature criterion is not sufficient. We also need $PE > P$ so that land glaciers will not
401 form at these locations. Figure 4b shows that the percent of land area with $PE > P$ increases
402 slightly with darkening of the land or increasing CO₂. Combining these criteria, Figure 4c shows
403 the percent of land area with $T_{max} > -2^{\circ}\text{C}$ and $PE > P$.

404 There are also some small areas of the *ocean*, all on coastlines, where the surface temperature
405 exceeds -2°C in the warmest month, but in all cases these areas represent less than 2% of the
406 ocean area (Table 2, Figure 4d).

407 With high-albedo land, the climate is so cold that very little of the land reaches above
408 freezing even with 200 ppm CO₂, as shown in Figure 4a. But with the warmer climate for darker
409 bare land (albedo 0.2), the above-freezing land area does become sensitive to the CO₂ level
410 (Figure 4e).

411

412 ***4.3 Refugia on desert land?***

413 Besides inhabiting the ends of narrow oceanic bays, photosynthetic eukaryotes may also have
414 been active on unglaciated land surfaces. Reviewing “early life on land”, Lenton and Daines
415 (2017) emphasized microbial mats powered by oxygenic photosynthesis. In their words:
416 “Initially, such mats would have been dominated by [prokaryotic] cyanobacteria. Sometime
417 during the Proterozoic Eon (2.5-0.54 Ga) they probably gained eukaryotic algae and fungi. . . .
418 Today a mixture of cyanobacteria, algae, fungi, lichens and nonvascular plants are found in
419 terrestrial mats, often termed ‘biological soil crusts’ or ‘cryptogamic cover’.” Lenton and Daines
420 cited evidence that “by the start of the Neoproterozoic (1 Ga), eukaryotes were probably present
421 alongside cyanobacteria in terrestrial mats, but whether these were algae is unclear.” The soil-
422 crust mats occur on modern midlatitude deserts that are seasonally above freezing, as in Utah and
423 Nevada. Similar environments may therefore have offered a habitat for mixed
424 prokaryotic/eukaryotic life in the deserts of Snowball Earth wherever the soil temperatures were
425 above freezing seasonally, as also proposed by Retallack (2023). The locations would have to be
426 in deserts ($PE > P$) to avoid burial by land-glaciers, but they could have received water from the
427 local sparse precipitation, or from runoff modulated through topography.

428

429 **5. Discussion and conclusion**

430 In our simulations we used the albedo of firn rather than glacier ice (Table 1) to represent the
431 snow-free parts of the frozen ocean, biasing the climate colder. Actual sea glaciers should have
432 had a slightly darker surface, allowing for a warmer climate. Yet, despite our conservative choice
433 of a brighter ice surface, our results suggest that a “hard” snowball climate with ice extending to
434 the equator could have allowed some locations to sustain the surface liquid water needed to host
435 photosynthetic life, despite extremely cold global-mean temperatures. Our global annual mean
436 surface temperatures \bar{T} are considerably colder than those of other GCMs simulating the hard-
437 snowball climate. Abbot et al. (2013) reviewed six GCMs; we can estimate \bar{T} from their Figure
438 1a for 100 ppm CO₂: for five GCMs, $\bar{T} \approx -38^\circ\text{C}$; the cold outlier (the FOAM GCM) had
439 $\bar{T} \approx -46^\circ\text{C}$. Our finding of above-freezing locations even with our extremely cold global mean
440 surface temperatures, all in the range -61 to -69°C (Table 1), thus argues strongly for refugia on
441 or near ocean bays.

442 Although we find strong evidence to support the potential for refugia, the distribution and
443 type of refugia (ice-surface or open-water) would be sensitive to the actual bare-land albedo. The
444 albedo of bare land surfaces during the Neoproterozoic may have been even darker than our
445 darkest case (albedo 0.2), as land plants had not yet evolved, which would limit the erosion of
446 rocks into smaller grain sizes, so that stony deserts, which have broadband albedo 0.10-0.15,
447 would be more likely than modern deserts of soil or sand. If Neoproterozoic land surfaces were
448 indeed dark like stony deserts, this lower land albedo would result in more refugia than we have
449 simulated here.

450 We find that modern nearly-enclosed bays, resulting from continental rifting (e.g. the
451 Red Sea), are especially habitable and could support seasonal refugia depending on the land
452 surface albedo. Since the dynamics of sea-glacier invasions into nearly-enclosed bays occur
453 below the resolution of the model simulations employed here (Campbell et al., 2011, 2014), our

454 results quantify the maximum potential for refugia within a hard-snowball climate with modern
455 continents; but the exact distribution of such nearly-enclosed bays on Neoproterozoic continents
456 would determine true habitability. A constriction at the entrance to the bay helps to slow the sea
457 glacier (Campbell et al., 2014), but the entrance must not be too shallow because ocean water
458 needs a path below the ice to reach the refugium. The strait at the entrance to the Red Sea (Bab el
459 Mandeb) is only 137 m deep (Siddall et al., 2002), so a sea glacier would likely become
460 grounded there.

461 Since Neoproterozoic continental reconstructions are constrained primarily by
462 paleomagnetism, which constrains the latitude but not the longitude, there remains large
463 uncertainty in the likelihood of large continental interiors, which we expect to strongly influence
464 our results (Merdith et al., 2021). The total land area was probably only slightly smaller than
465 today's (Hawkesworth et al., 2019), but the tropical bias in land distribution and degree of
466 continental "clumping", as well as the location and height of mountain ranges, could influence
467 our results (Laguë et al., 2023).

468 Our conclusion is that the ends of narrow oceanic bays were likely to serve as refugia for
469 photosynthetic eukaryotes, even during the coldest early phase of a snowball event.

470

471 ***Acknowledgments.***

472 This work was supported by NSF grant AGS-20-41491, and by a grant of time on NCAR
473 computers. MML acknowledges funding from the James S. McDonnell Foundation Postdoctoral
474 Fellowship in Dynamic and Multiscale Systems (grant # 220020576). We acknowledge helpful
475 discussions with Ursula Jongebloed, Bonnie Light, and Tyler Kukla. Figure 1 was drafted by
476 Richard Brandt.

477

478 ***Data availability statement.***

479 Model results are available through the University of Washington Libraries Dryad repository
480 (https://datadryad.org/stash/share/gpuwaesE07cQpgj_PwzewJaQdOLBSANcDtdSF_aK6hc).

481 Source code for CESM and SLIM, the models used in this study, are archived and publicly
482 accessible online (<https://doi.org/10.5281/zenodo.3895306>), with development code publicly
483 available on GitHub (https://escomp.github.io/CESM/release-cesm2/downloading_cesm.html)
484 for CESM.

485

486 ***Conflict of Interest Statement.***

487 The authors have no conflicts of interest to declare.

488

489 **Appendix.** *Penetration of a sea glacier down a narrow bay.*

490 A sea glacier entering a long narrow bay with length L_{bay} could be expected to have some
491 spatial and temporal variability in flow speed and thickness, due for example to obstructions
492 such as islands, shoals, or narrows in the bay; however, we can look beyond those possibly
493 minor variations to find characteristic numbers describing important aspects of long, straight,
494 narrow bays, their sea glaciers, and their climates.

495 We use a coordinate system $[x,y,z]$, with x and y horizontal; x can be aligned along the axis of
496 the bay, with $x=0$ at the bay mouth, and z is vertical. The corresponding velocity components are
497 $[u,v,w]$.

498 If a bay has a roughly uniform width W , then flow $v(x,y)$ transverse to the long axis of the
499 bay is small.

500 A sea glacier is floating, so except on shoals, there is no basal friction, and the flow speed
501 $u(x,y,z)$ along the bay can be treated as independent of depth, i.e. as $u(x,y)$.

502 Nye (1965) found a solution appropriate for $u(x,y)$ for floating ice in a uniform deep narrow
503 channel or deep bay, and Campbell et al. (2011) averaged Nye's solution across the bay to find
504 its average value $\bar{u}(x)$,

$$505 \quad \bar{u}(x) = \frac{W}{2} \frac{A(x)k(x)^n}{n+2}. \quad (1)$$

506 Temperature (and therefore ice softness) is incorporated in $A(x)$, resistive side-wall drag is
507 incorporated in $k(x)$, and $n \approx 3$ is the exponent in the Glen nonlinear flow law for ice (Glen, 1955).

508 Thomas (1973), and Sanderson (1979) showed that $\bar{u}(x)$ varies little in x , so following
509 Campbell et al. (2011) we set \bar{u} to be a constant, which we take as a characteristic velocity u_{char} .

510 Ablation rate $b(x)$ (m/s) depends on sublimation on the upper surface and melting at the base;
511 however, Goodman (2006) found that in the tropics on Snowball Earth, basal melting was
512 insignificant relative to surface sublimation. Although sublimation rate can vary along a long

513 narrow bay, following Campbell et al. (2011), we can define a characteristic ablation rate b_{char} as
 514 the average value of $b(x)$ along the centerline of the bay ($b < 0$ for sublimation).

515 A characteristic ice thickness H_{char} is set by the offshore sea glacier, which enters the bay and
 516 moves from its mouth at $x=0$ to the glacier terminus at $x=L_{glac}$ where the ice thickness reaches
 517 zero. Time t_{flow} for ice to travel the distance L_{glac} is inversely proportional to the speed u_{char} ; t_{flow}
 518 is also the time needed to sublimate the full ice thickness H_{char} at rate $-b_{char}$. Equating these two
 519 time estimates,

$$520 \quad t_{flow} = \frac{L_{glac}}{u_{char}} = \frac{H_{char}}{-b_{char}}. \quad (A2)$$

521 Solving Eq. (A2) for the penetration length L_{glac} in terms of the characteristic values,

$$522 \quad L_{term} = - (H_{char} u_{char}) / b_{char}. \quad (A3)$$

523 Eq. (A3) shows that penetration length L_{glac} is shorter when u_{char} is smaller (e.g. due to
 524 obstructions that impede ice flow along the bay), and when sublimation rate b_{char} is larger in
 525 magnitude (e.g. due to a warmer drier climate of the surrounding desert). Thickness H_{char} of the
 526 sea glacier on the adjacent ocean also matters; however, H_{char} is controlled by external factors
 527 beyond the narrow bay.

528 A characteristic steady-state thickness profile $h(x)$ can also be found. The volumetric flux
 529 $q(x)$ (m^3/s) is volume of incompressible ice passing through a “gate” across the bay with area W
 530 $h(x)$ at each position x , given by

$$531 \quad q(x) = u_{char} W h(x), \quad (A4)$$

532 and the mass-conservation equation takes the form

$$533 \quad dq/dx = W b_{char}. \quad (A5)$$

534 Putting Eq. (A4) into (A5) gives

$$535 \quad dh/dx = b_{char} / u_{char}. \quad (A6)$$

536 Integrating Eq. (A6) with the boundary condition $h(0) = H_{char}$ yields a linear thickness profile

537
$$h(x) = H_{char} + (b_{char}/u_{char}) x, \quad (A7)$$

538 and the sea glacier terminates where $h=0$, i.e. at L_{term} given in Eq. (A3) above.

539 Examples with greater spatial variability, fewer assumptions, and additional physical details
540 will be more complicated (e.g. see Campbell et al. (2011; 2014)); however, this simple analytical
541 solution can provide insights to guide refinements and approximations.

542 The existence of a refugium at the end of the bay requires $L_{glac} < L_{bay}$.

544

545 Abbot, D.S., Voigt, A., & Koll, D. (2011). The Jormungand global climate state and implications
546 for Neoproterozoic glaciations. *Journal of Geophysical Research: Atmospheres*, 116(D18),
547 D18103.

548 Abbot, D.S., Voigt, A., Li, D., Le Hir, G., Pierrehumbert, R.T., Branson, M., et al. (2013).
549 Robust elements of Snowball Earth atmospheric circulation and oases for life. *Journal of*
550 *Geophysical Research: Atmospheres*, 118(12), 6017-6027.

551 Abell, J.T., Pullen, A., Lebo, Z., Kapp, P., Gloege, L., Metcalf, A., et al. (2020a). A wind-
552 albedo-wind feedback driven by landscape evolution. *Nature Communications*.
553 <https://doi.org/10.1038/s41467-019-13661-w>

554 Abell, J.T., Rahimi, S.R., Pullen, A., Lebo, Z.J., Zhang, D., Kapp, P., et al. (2020b). A
555 quantitative model-based assessment of stony desert landscape evolution in the Hami Basin,
556 China: Implications for Plio-Pleistocene dust production in Eastern Asia," *Geophysical*
557 *Research Letters*, 47(20), e2020GL090064.

558 Benn, D.I., Le Hir, G., Bao, H., Donnadieu, Y., Dumas, C., Fleming, E.J., et al. (2015). Orbitally
559 forced ice sheet fluctuations during the Marinoan Snowball Earth glaciation. *Nature*
560 *Geoscience*, 8(9), 704-707.

561 Bitz, C.M., & Lipscomb, W.H. (1999). An energy-conserving thermodynamic model of sea ice.
562 *Journal of Geophysical Research: Oceans*, 104(C7), 15669-15677.

563 Bitz, C.M., Shell, K.M., Gent, P.R., Bailey, D.A., Danabasoglu, G., Armour, K.C., et al. (2012).
564 Climate Sensitivity in the Community Climate System Model Version 4, *J. Climate*, 25,
565 3053-3070, doi:10.1175/JCLI-D-11-00290.1

566 Bøggild, C.E., Brandt, R.E., Brown, K.J., & Warren, S.G. (2010). The ablation zone in northeast
567 Greenland: ice types, albedos and impurities. *Journal of Glaciology*, 56(195), 101-113.

568 Braun, C., Hörner, J., Voigt, A., & Pinto, J.G. (2022). Ice-free tropical waterbelt for Snowball
569 Earth events questioned by uncertain clouds. *Nature Geoscience*, 15(6), 489-493.

570 Budyko, M.I. (1969). The effect of solar radiation variations on the climate of the Earth. *Tellus*,
571 21, 611-619.

572 Campbell, A.J., Waddington, E.D., & Warren, S.G. (2011). Refugium for surface life on
573 Snowball Earth in a nearly-enclosed sea? A first simple model for sea-glacier invasion.
574 *Geophysical Research Letters*, 38(19), L19502. doi:10.1029/2011GL048846.

575 Campbell, A.J., Waddington, E.D., & Warren, S.G. (2014). Refugium for surface life on
576 Snowball Earth in a nearly-enclosed sea? A numerical solution for sea-glacier invasion
577 through a narrow strait. *J. Geophys. Res.*, 119, 2679-2690, doi:10.1002/2013JC009703.

578 Cess, R.D., Potter, G.L., Blanchet, J.P., Boer, G.J., Del Genio, A.D., Déqué, M., et al. (1990).
579 Intercomparison and interpretation of climate feedback processes in 19 atmospheric general
580 circulation models. *Journal of Geophysical Research: Atmospheres*, 95(D10), 16601-16615.

581 Conley, A.J., Lamarque, J.-F., Vitt, F., Collins, W.D., & Kiehl, J. (2013). PORT, a CESM tool
582 for the diagnosis of radiative forcing. *Geoscientific Model Development*, 6(2), 469-476.
583 <https://doi.org/10.5194/gmd-6-469-2013>

584 Crowley, T.J., & Baum, S.K. (1993). Effect of decreased solar luminosity on late Precambrian
585 ice extent. *Journal of Geophysical Research: Atmospheres*, 98(D9), 16723-16732.

586 Dadic, R., Mullen, P.C., Schneebeli, M., Brandt, R.E., & Warren, S.G. (2013). Effects of
587 bubbles, cracks, and volcanic tephra on the spectral albedo of bare ice near the Transantarctic
588 Mountains: Implications for sea glaciers on Snowball Earth. *Journal of Geophysical*
589 *Research: Earth Surface*, 118(3), 1658-1676.

590 Danabasoglu, G., Lamarque, J.-F., Bacmeister, J., Bailey, D., DuVivier, A., Edwards, J., et al.
591 (2020). The community earth system model version 2 (CESM2). *Journal of Advances in*
592 *Modeling Earth Systems*, 12(2), e2019MS001916. <https://doi.org/10.1029/2019MS001916>
593 Donnadieu, Y., Fluteau, F., Ramstein, G., Ritz, C., & Besse, J. (2003). Is there a conflict between
594 the Neoproterozoic glacial deposits and the snowball Earth interpretation: an improved
595 understanding with numerical modeling. *Earth and Planetary Science Letters*, 208(1), 101-
596 112.

597 Evans, D.A.D. (2000). Stratigraphic, geochronological, and paleomagnetic constraints upon the
598 Neoproterozoic climatic paradox. *American Journal of Science*, 300(5), 347-433.

599 Glen, J. (1955), The creep of polycrystalline ice, *Proc. R. Soc. A*, 228, 519–538.

600 Goodman, J.C. (2006). Through thick and thin: Marine and meteoric ice in a "Snowball Earth"
601 climate. *Geophysical Research Letters*, 33, L16701. doi:10.1029/2006GL026840

602 Goodman, J.C., & Pierrehumbert, R.T. (2003). Glacial flow of floating marine ice in "Snowball
603 Earth". *J. Geophys. Res. Oceans*, 108(C10), 3308. <https://doi.org/10.1029/2002JC001471>

604 Grenfell, T.C., Warren, S.G., and Mullen, P.C. (1994). Reflection of solar radiation by the
605 Antarctic snow surface at ultraviolet, visible, and near-infrared wavelengths. *J. Geophys.*
606 *Res.*, 99, 18669-18684.

607 Harland, W.B. (1964). Critical evidence for a great infra-Cambrian glaciation. *Geologische*
608 *Rundschau*, 54(1), 45-61.

609 Hawkesworth, C., Cawood, P.A., & Dhuime, B. (2019). Rates of generation and growth of the
610 continental crust. *Geoscience Frontiers*, 10, 165-173.

611 Hörner, J., & Voigt, A. (2023). Sea-ice thermodynamics can determine waterbelt scenarios for
612 Snowball Earth. *EGUSphere*, doi:10.5194/egusphere-2023-2073.

613 Hoffman, P.F., & Schrag, D.P. (2000). Snowball Earth. *Scientific American*, 68(1), 68-75.

614 Hoffman, P.F., & Schrag, D.P. (2002). The Snowball Earth hypothesis: Testing the limits of
615 global change. *Terra Nova*, 14, 129-155.

616 Hoffman, P.F., Abbot, D.S., Ashkenazy, Y., Benn, D.I., Brocks, J.J., Cohen, P.A., et al. (2017).
617 Snowball Earth climate dynamics and Cryogenian geology-geobiology. *Science Advances*,
618 3(11), e1600983. doi: 10.1126/sciadv.1600983

619 Hudson, S.R., Warren, S.G., Brandt, R.E., Grenfell, T.C., & Six, D. (2006). Spectral
620 bidirectional reflectance of Antarctic snow: Measurements and parameterization. *Journal of*
621 *Geophysical Research: Atmospheres*, 111, D18106. <https://doi.org/10.1029/2006JD007290>

622 Hunke, E., Lipscomb, W.H., Turner, A., Jeffery, N., & Elliott, S. (2015). *CICE: the Los Alamos*
623 *Sea Ice Model documentation and software user's manual LA-CC-06-012*. Los Alamos
624 National Laboratory, Los Alamos, New Mexico.

625 Kenrick, P., Wellman, C.H., Schneider, H., & Edgecombe, G.D. (2012). A timeline for
626 terrestrialization: consequences for the carbon cycle in the Palaeozoic. *Phil. Trans. Royal*
627 *Soc. London*, B367(1588), 519–536.

628 Kirschvink, J.L. (1992) Late Proterozoic low-latitude global glaciation: the Snowball Earth, in
629 *The Proterozoic Biosphere*, Schopf, J.W., and Klein, C. eds., pp. 51-52, Cambridge Univ.
630 Press, New York.

631 Knoll, A.H. (2011). The Multiple Origins of Complex Multicellularity. *Annual Review of Earth*
632 *and Planetary Sciences*, 39(1), 217-239.

633 Knoll, A.H. (2014). Paleobiological perspectives on early eukaryotic evolution. *Cold Spring*
634 *Harbor Perspectives in Biology*, 6(1), a016121.

635 Laguë, M.M., Bonan, G.B., & Swann, A.L.S. (2019). Separating the impact of individual land
636 surface properties on the terrestrial surface energy budget in both the coupled and uncoupled
637 land–atmosphere system. *Journal of Climate*, 32(18), 5725-5744.

638 Laguë, M.M., Quetin, G.R., Ragen, S., & Boos, W.R. (2023). Continental configuration controls
639 the base-state water vapor greenhouse effect: lessons from half-land, half-water planets.
640 *Climate Dynamics*, <https://doi.org/10.1007/s00382-023-06857-w>
641 Lenton, T.M., & Daines, S.J. (2017). Matworld – the biogeochemical effects of early life on
642 land. *New Phytologist*, *215*, 531-537, doi:10.1111/nph.14338.
643 Lewis, J.P., Weaver, A.J., & Eby, M. (2006). Deglaciating the snowball Earth: Sensitivity to
644 surface albedo. *Geophysical Research Letters*, *33*(23), L23604. doi:10.1029/2006GL027774
645 Li, D., & Pierrehumbert, R.T. (2011). Sea glacier flow and dust transport on Snowball Earth.
646 *Geophysical Research Letters*, *38*(17), L17501.
647 Liu, Y., Peltier, W.R., Yang, J., & Vettoretti, G. (2013). The initiation of Neoproterozoic
648 "snowball" climates in CCSM3: the influence of paleocontinental configuration. *Climate of*
649 *the Past*, *9*(6), 2555-2577.
650 Liu, Y., Peltier, W.R., Yang, J., Vettoretti, G., & Wang, Y. (2017). Strong effects of tropical ice-
651 sheet coverage and thickness on the hard snowball Earth bifurcation point. *Climate*
652 *Dynamics*, *48*(11), 3459-3474.
653 Liu, Y., Peltier, W.R., Yang, J., and Hu, Y. (2018). Influence of surface topography on the
654 critical carbon dioxide level required for the formation of a modern Snowball Earth. *Journal*
655 *of Climate*, *31*(20), 8463-8479.
656 Liu, P., Liu, Y., Peng, Y., Lamarque, J.-F., Wang, M., & Hu, Y. (2020). Large influence of dust
657 on the Precambrian climate. *Nature Communications*, *11*(1) 4427.
658 Liu, Y., Liu, P., Li, D., Peng, Y., & Hu, Y. (2021). Influence of dust on the initiation of
659 Neoproterozoic Snowball Earth events. *Journal of Climate*, *34*(16) 6673-6689.
660 Macdonald, F.A., Schmitz, M.D., Crowley, J.L., Roots, C.F., Jones, D.S., Maloof, A.C., et al.
661 (2010). Calibrating the Cryogenian. *Science*, *327*(5970), 1241-1243.
662 McKay, C.P. (2000). Thickness of tropical ice and photosynthesis on a snowball Earth.
663 *Geophysical Research Letters*, *27*(14), 2153-2156.
664 Merdith, A.S., Williams, S.E., Collins, A.S., Tetley, M.G., Mulder, J.A., Blades, M.L., et al.
665 (2021). Extending full-plate tectonic models into deep time: Linking the Neoproterozoic and
666 the Phanerozoic. *Earth-Science Reviews*, *214*, 103477.
667 Monteith, J.L. (1981). Evaporation and surface temperature. *Quart. J. Roy. Meteor. Soc.*, *107*, 1-
668 27.
669 Morris, J.L., Puttick, M.N., Clark, J.W., Edwards, D., Kenrick, P., Pressel, S., et al. (2018). The
670 timescale of early land plant evolution. *Proc. Nat. Acad. Sci. USA*, *115* (10), E2274-E2283.
671 doi:10.1073/pnas.1719588115.
672 Neale, R.B., Richter, J.H., Conley, A.J., Park, S., Lauritzen, P.H., Gettelman, A. Williamson,
673 D.L., et al. (2010). *Description of the NCAR Community Atmosphere Model (CAM 4.0)*
674 (NCAR/Tn-485+Str), National Center for Atmospheric Research, Boulder, Colorado.
675 Nye, J. F. (1965), The flow of a glacier in a channel of rectangular, elliptical or parabolic cross-
676 section, *J. Glaciol.*, *5*, 661–690.
677 Penman, H.L. (1948). Natural evaporation from open water, bare soil and grass. *Proc. Roy. Soc.*
678 *London*, *193A*, 120-145.
679 Pierrehumbert, R. T. (2005). Climate dynamics of a hard snowball Earth. *J. Geophys. Res.*
680 *Atmos.*, *110*, D01111, doi:10.1029/2004JD005162.
681 Pollard, D., & Kasting, J.F. (2004) Climate-ice sheet simulations of Neoproterozoic glaciation
682 before and after collapse to Snowball Earth, in *The Extreme Proterozoic: Geology,*
683 *Geochemistry, and Climate*, *Geophys. Monogr. Ser.*, vol. 146, edited by G. Jenkins et al., pp
684 91-105, AGU, Washington, D.C.

685 Pollard, D., & Kasting, J.F. (2005). Snowball Earth: A thin-ice solution with flowing sea
686 glaciers. *J. Geophys. Res.*, *110*, C07010, doi:10.1029/2004JC002525.

687 Pollard, D., Kasting, J.F. & Zutter, M.E. (2017). Snowball Earth: Asynchronous coupling of
688 sea-glacier flow with a global climate model. *J. Geophys. Res. Atmos.*, *122*, 5157-5171,
689 doi:10.1002/2017JD026621.

690 Porter, S.M. (2004). The fossil record of early eukaryotic diversification. *The Paleontological*
691 *Society Papers*, *10*, 35–50.

692 Retallack, G.J. (2023). Neoproterozoic Snowball Earth extent inferred from paleosols in
693 California. *J. Palaeosciences*, *72*, 9-28, doi:10.54991/jop.2023.1851.

694 Sanderson, T. J. O. (1979), Equilibrium profile of ice shelves, *J. Glaciol.*, *22*, 435–460.

695 Scheff, J., & Frierson, D.M.W. (2014). Scaling potential evapotranspiration with greenhouse
696 warming. *Journal of Climate*, *27*(4), 1539-1558.

697 Schrag, D.P., Berner, R.A., Hoffman, P.F., & Halverson, G.P. (2002). On the initiation of a
698 snowball Earth. *Geochemistry, Geophysics, Geosystems*, *3*(6) 1-21.
699 <https://doi.org/10.1029/2001GC000219>

700 Sellers, W.D. (1969). A global climatic model based on the energy balance of the earth-
701 atmosphere system. *Journal of Applied Meteorology and Climatology*, *8*(3), 392-400.

702 Sejas, S.A., Taylor, P.C. & Cai, M. (2018). Unmasking the negative greenhouse effect over the
703 Antarctic Plateau. *npj Clim Atmos Sci* *1*, 17.

704 Siddall, M., Smeed, D., Matthiesen, S., & Rohling, E. (2002). Modelling the seasonal cycle of
705 the exchange flow in Bab el Mandab (Red Sea). *Deep Sea Research Part I*, *49*(9), 1551-
706 1569.

707 Smith, E.A. (1986). The structure of the Arabian heat low. Part I: Surface energy budget.
708 *Monthly Weather Review*, *114*(6), 1067-1083.

709 Thomas, R. H. (1973), The creep of ice shelves: Theory, *J. Glaciol.*, *12*, 45–53.

710 Vincent, W.F. & Howard-Williams, C. (2000). Life on Snowball Earth. *Science*, *287*(5462),
711 2421-2421.

712 Vincent, W.F., Gibson, J.A.E., Pienitz, R., Villeneuve, V., Broady, P.A., Hamilton, P.B., &
713 Howard-Williams, C. (2000). Ice Shelf Microbial Ecosystems in the High Arctic and
714 Implications for Life on Snowball Earth. *Naturwissenschaften*, *87*(3), 137-141.

715 Voigt, A., & Abbot, D.S. (2012). Sea-ice dynamics strongly promote Snowball Earth initiation
716 and destabilize tropical sea-ice margins. *Climate of the Past*, *8*(6), 2079-2092.

717 Voigt, A., & Marotzke, J. (2010). The transition from the present-day climate to a modern
718 Snowball Earth. *Climate Dynamics*, *35*(5), 887-905.

719 Voigt, A., Abbot, D.S., Pierrehumbert, R.T., & Marotzke, J. (2011). Initiation of a Marinoan
720 Snowball Earth in a state-of-the-art atmosphere-ocean general circulation model. *Climate of*
721 *the Past*, *7*(1), 249-263.

722 Walsh, A., Ball, T., & Schultz, D.M. (2019). Extreme sensitivity in Snowball Earth formation to
723 mountains on PaleoProterozoic supercontinents. *Scientific Reports*, *9*(1), 2349.

724 Warren, S.G., & Brandt, R.E. (2006). Comment on “Snowball Earth: A thin-ice solution with
725 flowing sea glaciers” by David Pollard and James F. Kasting. *Journal of Geophysical*
726 *Research*, *111*, C09016.

727 Warren, S.G., Brandt, R.E., Grenfell, T.C., & McKay, C.P. (2002). Snowball Earth: Ice thickness
728 on the tropical ocean. *J. Geophys. Res.*, *107*(C10), 3167.

729 Yang, J., Peltier, W.R., & Hu, Y. (2012). The initiation of modern soft and hard Snowball Earth
730 climates in CCSM4. *Climate of the Past*, *8*(3) 907-918.

731

732 *Tables*

733

734 **Table 1.** Band-albedos of representative snow, ice, and land surfaces. The spectral albedos for

735 four of these surface types are shown in Figure 1.

736

Surface type	Albedo			Reference
	0.3-0.7 μm (UV, visible)	0.7-3.0 μm (near-infrared)	0.3-3.0 μm (total solar; broadband)	
Snow	0.98	0.68	0.83	Hudson et al. (2006), Grenfell et al. (1994)
Firn	0.94	0.44	0.69	Dadic et al. (2013)
Glacier ice	0.89	0.26	0.58	Dadic et al. (2013)
Polar desert (gravel and soil of northeast Greenland)	0.13	0.21	0.17	Bøggild et al. (2010)
Sand desert (Arabia)			0.40	Smith (1986)
Stony desert (Gobi)			0.10-0.15	Abell (2020ab)

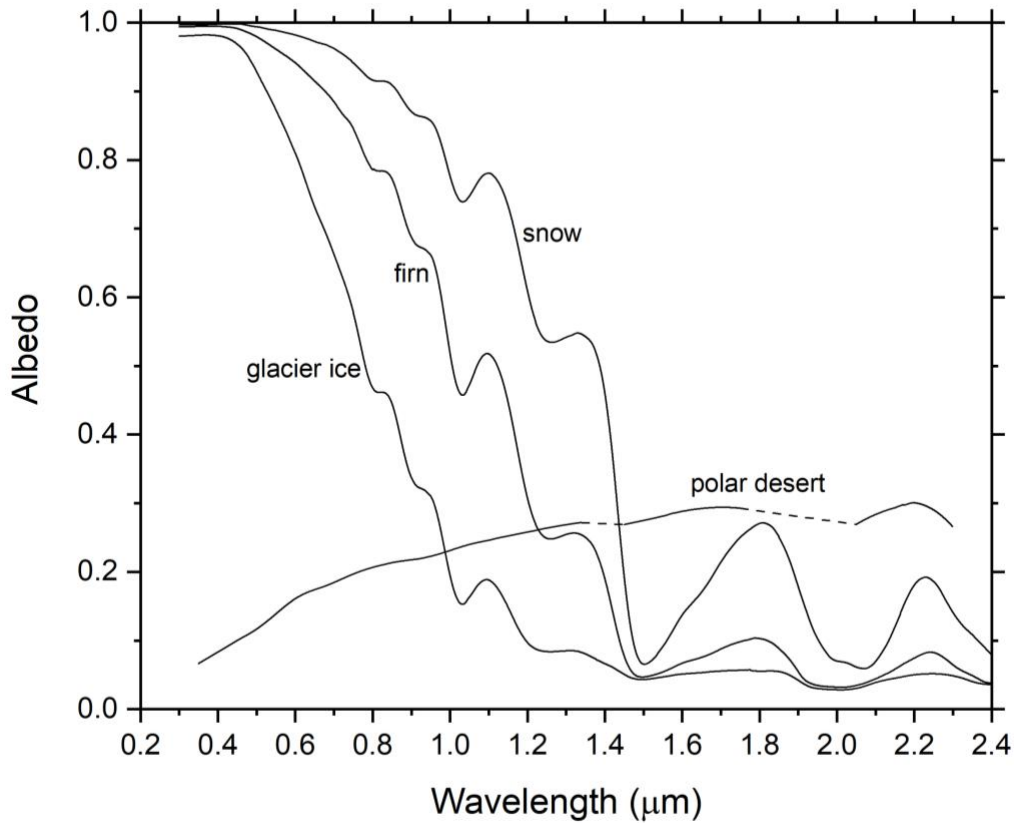
737

738
739
740
741

Table 2. Characteristics of the model runs. The consequences of radiative forcing shown for combinations of changes to the bare-land albedo and the CO₂ level are relative to the coldest case of CO₂ = 10 ppm and bare-land albedo = 0.4 broadband (0.3 visible / 0.5 near-IR). Land is “net-evaporative” if potential evaporation (PE) exceeds precipitation (P).

Albedo of bare (snow-free) land		CO ₂ (ppm)	Global average planetary albedo	Global mean surface temperature (°C)	Radiative forcing (W m ⁻²) relative to 10 ppm, albedo 0.4	Percent of land area with $T_{max} > -2^{\circ}\text{C}$ in warmest month	Percent of land area with $PE > P$ in annual mean	Percent of land area with $PE > P$ and $T_{max} > -2^{\circ}\text{C}$	Percent of ocean area with $T_{max} > -2^{\circ}\text{C}$ in warmest month
Broadband solar	Visible/near-IR								
0.4	0.3/0.5	10	0.683	-69.2	0	0.1	50.8	0.1	0
0.4	0.3/0.5	50	0.681	-67.9	2.75	0.23	54.16	0.23	0.01
0.4	0.3/0.5	200	0.68	-66.5	5.16	0.54	59.83	0.54	0.04
0.35	0.25/0.45	50	0.675	-66.6	3.78	1.41	57.67	1.41	0.11
0.3	0.2/0.4	10	0.67	-66.7	2.05	3.1	56.77	3.1	0.24
0.3	0.2/0.4	25	0.669	-66.0	3.6	3.48	59.9	3.45	0.31
0.3	0.2/0.4	50	0.668	-65.3	4.8	4.04	63.14	4.04	0.36
0.3	0.2/0.4	100	0.667	-64.6	5.99	5.27	66.32	5.27	0.49
0.3	0.2/0.4	200	0.667	-63.9	7.21	5.72	70.4	5.7	0.40
0.25	0.15/0.35	50	0.662	-64.0	5.81	9.15	68.16	9.02	0.87
0.2	0.1/0.3	10	0.657	-64.2	4.06	12.15	67.87	12.02	1.17
0.2	0.1/0.3	50	0.655	-62.7	6.81	14.99	74.57	14.82	1.53
0.2	0.1/0.3	200	0.653	-61.2	9.22	17.22	85.03	17.05	1.83

742



744

745

Figure 1. Spectral albedos of representative surface types. Cold fine-grained snow was measured

746

at Dome C on the East Antarctic Plateau (Figure 6 of Hudson et al., 2006). Firn was measured

747

just upstream of the Allan Hills blue-ice field in East Antarctica (Site R9 of Dadic et al., 2013).

748

Glacier ice is from the Allan Hills blue-ice field (Site R1 of Dadic et al., 2013). These firn and

749

ice sites can represent sea-glacier surfaces on Snowball Earth because they were originally

750

formed by snow accumulation and exposed by sublimation, never having experienced melting.

751

The "polar desert" site is an unvegetated surface of soil and stones in northeast Greenland

752

(photograph shown in Figure 6 of Bøggild et al., 2010). For the "polar desert" surface, albedo

753

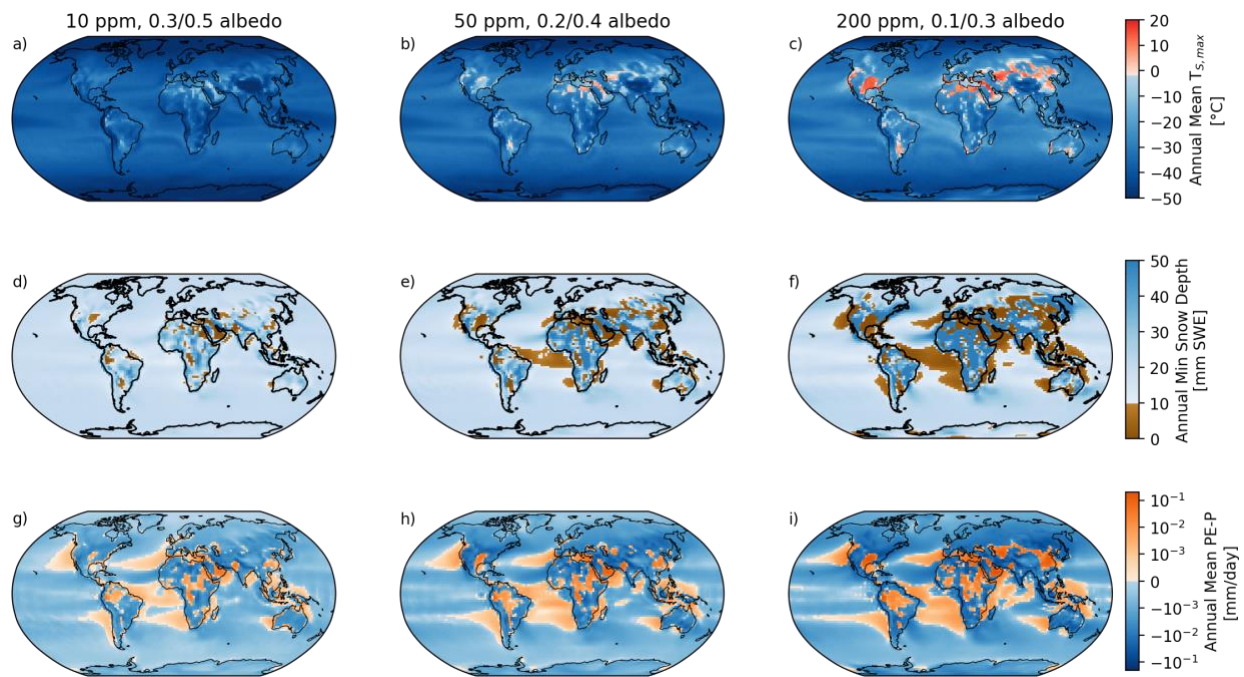
measurements were not possible from 1.35 to 1.45 μm , and from 1.75 to 2.05 μm , because the

754

incident solar radiation flux was near zero at these wavelengths due to atmospheric water-vapor

755

absorption; the dashed lines interpolate across these regions.



756

757

758

Figure 2. Habitability of the simulated snowball climate. **(a, b, c)** Surface temperature of the

759

warmest month in the coldest simulated case (10 ppm CO₂, bare-land albedo 0.4), the midpoint

760

simulation (50 ppm CO₂, bare-land albedo 0.3) and the warmest case (200 ppm CO₂, bare-land

761

albedo 0.1), respectively. Red areas indicate locations with seasonal melting, suggesting the

762

possibility of ice-surface refugia. **(d, e, f)** Annual minimum snow depth (monthly mean) from the

763

same cases, given as mm snow water equivalent (SWE), which is equivalent to kg/m². Brown

764

areas indicate places where snow depth drops below the threshold for surface-albedo change at

765

some point during the year. Note that ocean areas without snow accumulation would nonetheless

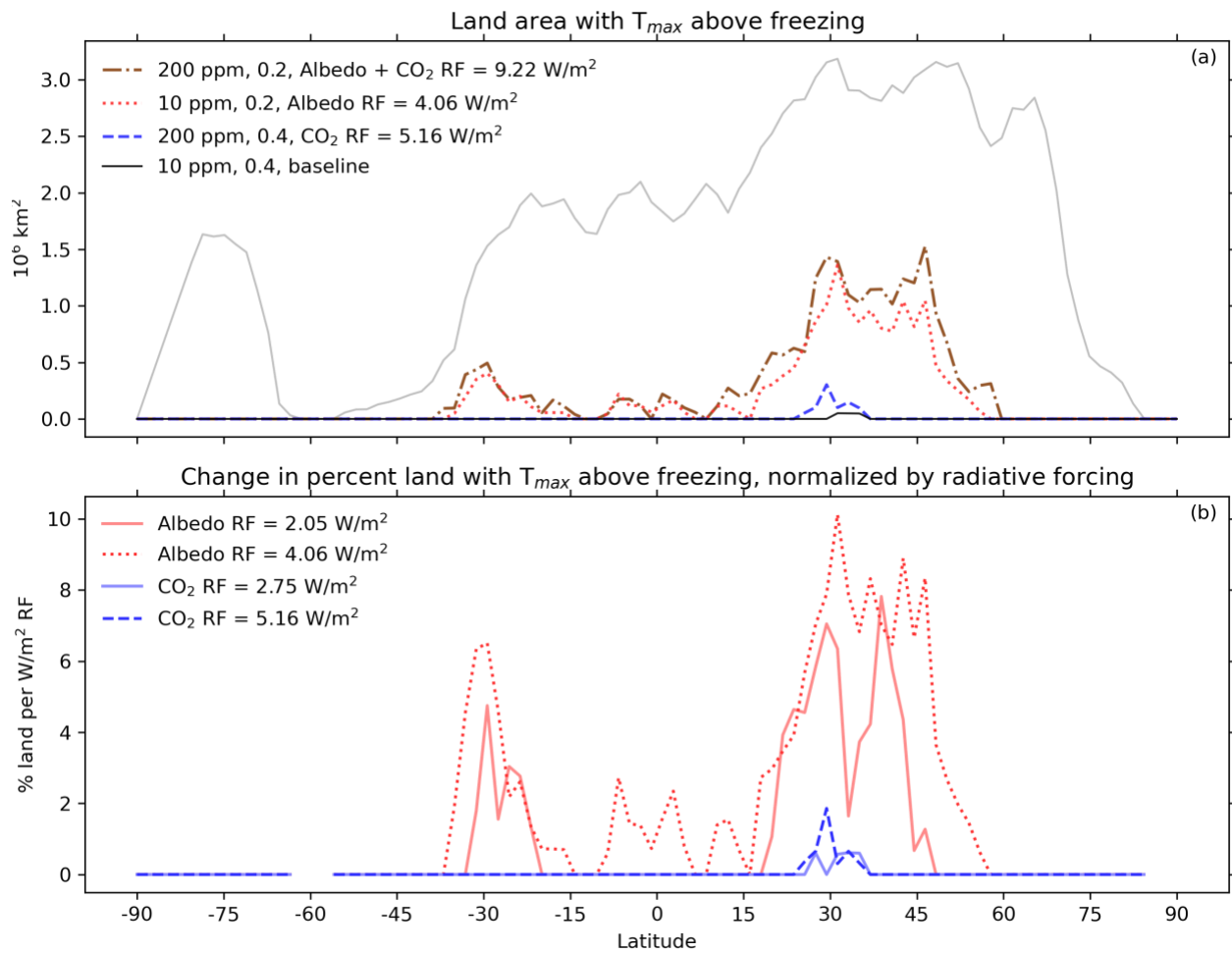
766

be covered by sea glaciers. **(g, h, i)** Annual mean potential evaporation (PE) minus precipitation

767

(P) for the same cases.

768



769

770 **Figure 3.** (a) Area of land (per 1.9 degrees of latitude increment) with temperature above
 771 freezing in the warmest month. Total land area is shown in grey. (b) Change in percent land area
 772 above freezing in the warmest month, per unit radiative forcing, relative to the coldest case
 773 (10 ppm CO₂, albedo 0.4).

774

775

776

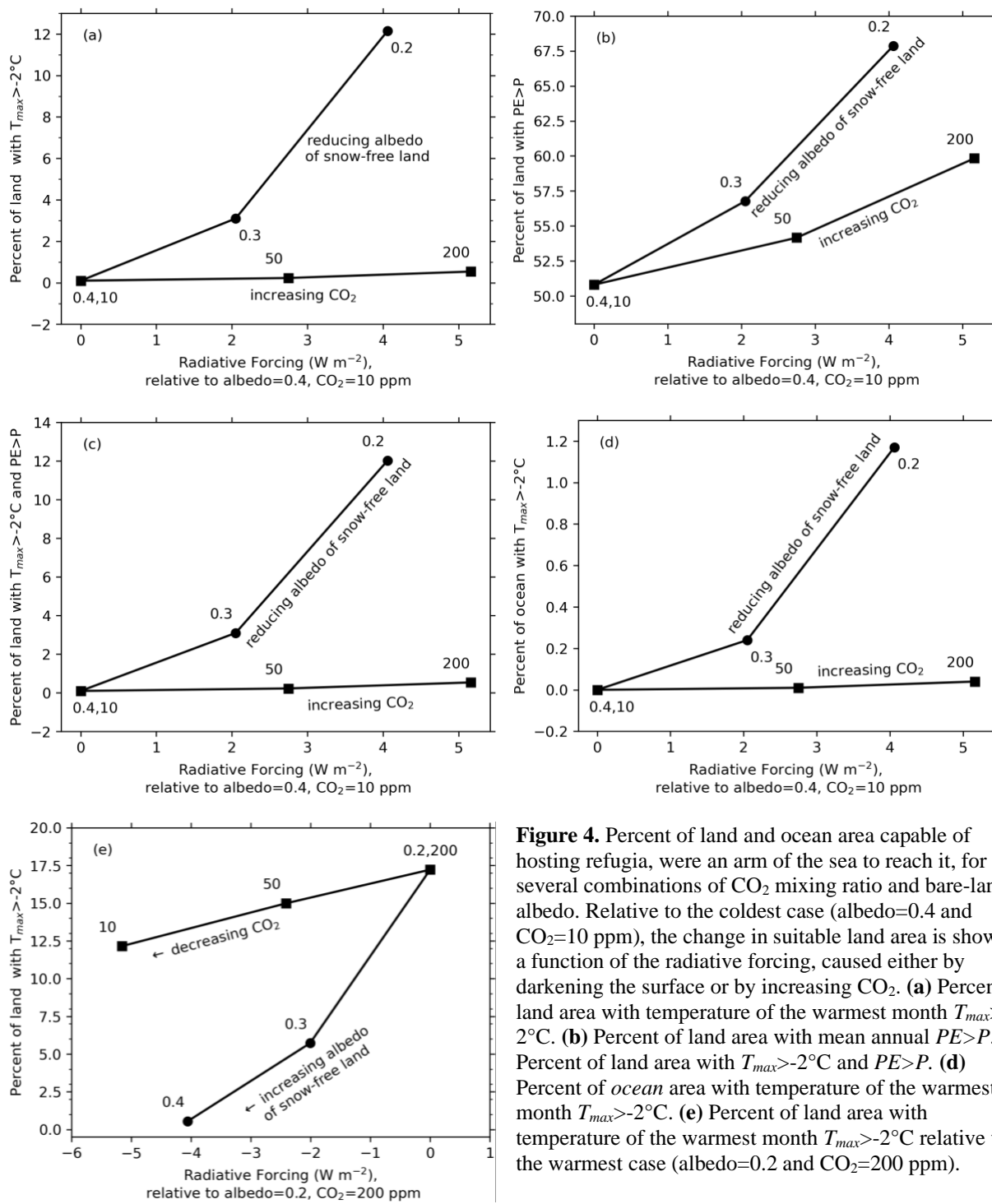


Figure 4. Percent of land and ocean area capable of hosting refugia, were an arm of the sea to reach it, for several combinations of CO_2 mixing ratio and bare-land albedo. Relative to the coldest case (albedo=0.4 and $CO_2=10$ ppm), the change in suitable land area is shown as a function of the radiative forcing, caused either by darkening the surface or by increasing CO_2 . **(a)** Percent of land area with temperature of the warmest month $T_{max} > -2^\circ C$. **(b)** Percent of land area with mean annual $PE > P$. **(c)** Percent of land area with $T_{max} > -2^\circ C$ and $PE > P$. **(d)** Percent of ocean area with temperature of the warmest month $T_{max} > -2^\circ C$. **(e)** Percent of land area with temperature of the warmest month $T_{max} > -2^\circ C$ relative to the warmest case (albedo=0.2 and $CO_2=200$ ppm).

777
778

779
780

